Chapter 7

Forced Turbulent Heat Convection in a Rectangular Duct with Non-Uniform Wall Temperature

G.A. Rivas, E.C. Garcia and M. Assato

Additional information is available at the end of the chapter

http://dx.doi.org/10.5772/52394

1. Introduction

Rectangular ducts are widely used in heat transfer devices, for instance, in compact heat exchangers, gas turbine cooling systems, cooling channels in combustion chambers and nuclear reactors. Forced turbulent heat convection in a square or rectangular duct is one of the fundamental problems in the thermal science and fluid mechanics. Recently, Qin and Fletcher [1] showed that Prandtl's secondary flow of the second kind has a significant effect in the transport of heat and momentum, as revealed by the recent Large Eddy Simulation (LES) technique. Several experimental and numerical studies have been conducted on turbulent flow though of non-circular ducts: Nikuradse [2]; Gessner and Emery [3]; Gessner and Po [4]; Melling and Whitelaw [5]; Nakayama et al. [6]; Myon and Kobayashi [7]; Assato [8]; Assato and De Lemos [9]; Home et al. [10]; Luo et al. [11]; Ergin et al. [12] Launder and Ying [13]; Emery et al. [14]; Hirota et al.[15]; Rokni [16]; Hongxing [17]; Yang and Hwang [18]; Park [19];Zhang et al. [20]; Zheng et al. [21]; Su and Da Silva Neto [22]; Saidi and Sundén [23]; Rokni [24]; Valencia [25]; Sharatchandra and Rhode [26]; Campo et al. [27]; Rokni and Sundén [28]; Yang and Ebadian [29] and others. The Melling and Whitelaw´s [5] experimental work shows characteristics of turbulent flow in a rectangular duct where they have been used a laser-Doppler anemometer in which report the axial development mean velocity, secondary mean velocity, etc. Nakayama et al. [6] show the analysis of the fully developed flow field in rectangular and trapezoidal cross-section ducts; finite difference method was implemented and the model of Launder and Ying [13] has been used. On the other hand, Hirota et al. [15] present an experimental work in turbulent heat transfer in square ducts; they show details of turbulent flows and temperature fields. Likewise, Rokni [16] carried out a comparison of four different turbulence models for predicting the turbulent Reynolds stresses, and three turbulent heat flux models for square ducts. The literature

presents various turbulence modeling in which confirm Linear Eddy Viscosity Models (LEVM) can give inaccurate predictions for Reynolds normal stresses: it does not have ability to predict secondary flows in non-circular ducts due to its isotropic treatment. In spite of that, they is one of the most popular model in the engineering due to its simplicity, good numerical stability in which can be applied in a wide variety of flows. Thus, the Nonlinear Eddy Viscosity Model (NLEVM) represents a progress of the classical LEVM in which this last one gives inequality treatment of the Reynolds normal stresses, needs of conditions for calculating turbulence-driven secondary flow in non-circular ducts and it has relatively high cost for solving the necessary two-equation formulation. The Reynolds Stress Model (RSM), also called second order or second moment closure model, is very accurate in the calculation of mean flow properties and Reynolds stresses, for simple to more complex flows including wall jets, asymmetric channel, non-circular duct and curved flows. However, RSM has some disadvantages, such as, very large computing costs. For calculating the turbulent heat fluxes, the Simple Eddy Diffusivity (SED) and Generalized Gradient Diffusion Hypothesis (GGDH) models have been adopted and investigated. Most of the works presented in the literature show results assuming constant temperature on the wall. However, in many engineering applications the heat fluxes and surface temperatures are non-constants around the duct, therefore becoming important the knowledge of the variation of the conductance around the duct, according to Kays and Crawford [30]. According to Garcia´s developments [31], it is possible to carry out analysis with non-constant wall temperature boundary conditions. In this case, it is necessary to define a value that represents the mean wall temperatures in a given cross section, in which he has named T_{Wm}. Following this treatment, for the present paper, important results have been computed and they are here being presented for rectangular cross-section ducts. Fluids such as air and water were analyzed under the influence of non-constant wall temperature distributions, with consequent presentations of resulted about turbulent convective heat exchanges and flow temperature profiles.

2. Mathematical formulation

2.1. Governing equations

The Reynolds Averaged Navier Stokes (RANS) equation system is composed of: continuity equation (1), momentum equation (2), and energy equation (3).

$$\frac{\partial}{\partial x_j}(U_j) = 0 \tag{1}$$

$$\frac{\partial}{\partial x_j}(U_i U_j) = -\frac{1}{\rho}\frac{\partial P}{\partial x_i} + \frac{1}{\rho}\frac{\partial}{\partial x_j}\left[\mu\left(\frac{\partial U_i}{\partial x_j} + \frac{\partial U_j}{\partial x_i}\right)\right] + \frac{1}{\rho}\frac{\partial}{\partial x_j}(-\rho\overline{u_i' u_j'}) \tag{2}$$

$$\frac{\partial}{\partial x_j}\left(U_j T_f\right) = \frac{1}{\rho}\frac{\partial}{\partial x_j}\left[\frac{\mu}{\mathrm{Pr}}\frac{\partial T_f}{\partial x_j} + \left(-\rho\overline{u_j' t'}\right)\right] \tag{3}$$

For analyses of fully developed turbulent flow and heat transfer, the following hypothesis has been adopted: steady state, condition of non-slip on the wall and fluid with constant properties. The turbulent Reynolds stress $(-\rho\overline{u_i' u_j'})$ and the turbulent heat flux $(-\rho\overline{u_j' t'})$ were modeled and solved by algebraic and/or differential expressions.

2.2. Turbulence models for reynolds stresses

2.2.1. Nonlinear Eddy Viscosity Model (NLEVM)

The NLEVM Model to reproduce the tensions of Reynolds, it is necessary to include non-linear terms in the basic constitutive equations. This is done by attempting to capture the sensitivity of the curvatures of the stream lines. This model is based on the initial proposal of Speziale [35]. The Reynolds average equations, Equations (1) to (3), are applied for the device presents in the Figure 1(a) and (b).

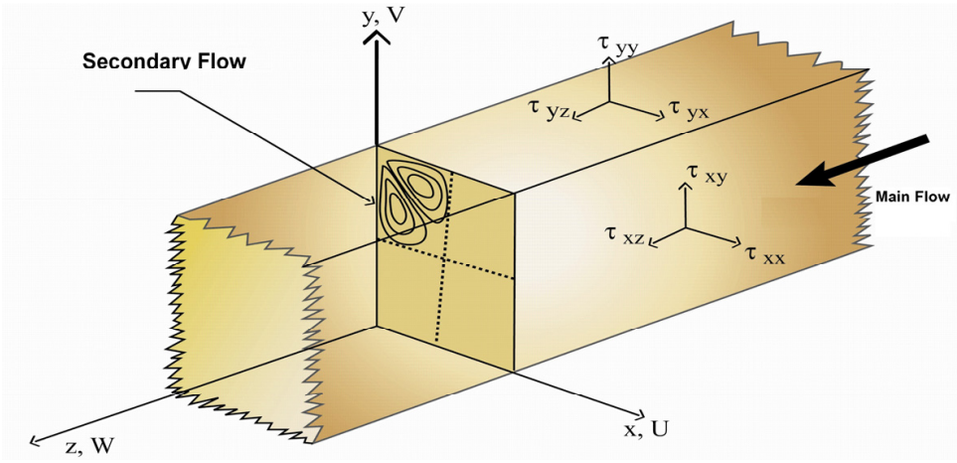

(a)

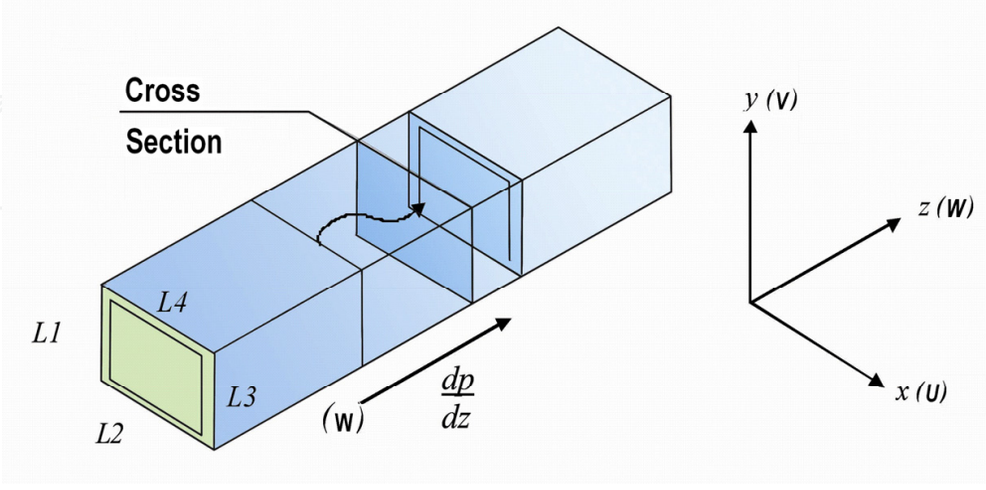

(b)

Figure 1. (a) Fully developed turbulent flows in rectangular ducts, (b) Rectangular duct: reference system and transversal section.

The velocity components *U and V* represent the secondary flow, and the axial velocity component *W*, the velocity of the main flow. The transport equations in tensorial form for the turbulent kinetic energy, κ, and the rate of dissipation ε, respectively, they are given by:

$$U_i \frac{\partial k}{\partial x_i} = \frac{\partial}{\partial x_i}\left(\frac{\mu_t}{\rho \sigma_k} \frac{\partial k}{\partial x_i} \right) + P_k - \varepsilon \tag{4}$$

$$U_i \frac{\partial \varepsilon}{\partial x_i} = \frac{\partial}{\partial x_i}\left(\frac{\mu_t}{\rho \sigma_\varepsilon} \frac{\partial \varepsilon}{\partial x_i} \right) + c_1 \frac{\varepsilon}{k} P_k - c_2 f_2 \frac{\varepsilon^2}{k} \tag{5}$$

The symbols P_k and μ_t, represent the rate of the turbulent kinetic energy production and the turbulent viscosity, respectively, are expressed by:

$$P_k = \tau_{ij} \frac{\partial U_i}{\partial x_j}, \; \mu_t = c_\mu f_\mu \rho \frac{k^2}{\varepsilon} \tag{6}$$

In the present work for NLEVM, the formulations of Low Reynolds Number will be assumed for wall treatment. The damping functions f_2 and f_μ observed in Equations (5) and (6) were proposed by Abe et al [36]. These functions and the constant c_1 and c_2 are used in equations $k-\varepsilon$. The subscript *P* refers to the nodal point near to the wall. Thus U_P and k_P are the values of the velocity and kinetic energy in this point, respectively. For the constants c_μ, c_1, c_2, σ_k and σ_ε are assumed the values of 0.09; 1.5; 1.9; 1.4 e 1.3; respectively. New constitutive relation for the tensions of Reynolds in the NLEVM model was assumed in according to the thesis of Assato [8]:

$$\tau_{ij} = \left(\mu_t S_{ij} \right)^{L} + \left(c_{1NL} \mu_t \frac{k}{\varepsilon} \left[S_{ik} S_{kj} - \tfrac{1}{3} S_{kl} S_{kl} \delta_{ij} \right] \right)^{NL} \tag{7}$$

This expression shows that the second term of the right side in Equation (7) represents the nonlinear relation added the original constitutive relation. This quadratic term represents the degree of anisotropy between the normal tensions of Reynolds responsible for predicting the secondary flow in non circular ducts. The values of c_{1NL} proposed by Speziale [35] is equal to 1.68. In this work, c_{1NL} will be analyzed and will adopt values for the formulation of Low Reynolds Numbers. The normal and shear tensions of Reynolds are expressed as:

$$\tau_{xx} = c_{1NL} \mu_t \frac{k}{\varepsilon} \left[\frac{1}{3} \left(\frac{\partial W}{\partial x} \right)^2 - \frac{2}{3} \left(\frac{\partial W}{\partial y} \right)^2 \right]; \; \tau_{yy} = c_{1NL} \mu_t \frac{k}{\varepsilon} \left[\frac{1}{3} \left(\frac{\partial W}{\partial y} \right)^2 - \frac{2}{3} \left(\frac{\partial W}{\partial x} \right)^2 \right] \tag{8}$$

$$\tau_{xy} = c_{1NL} \mu_t \frac{k}{\varepsilon} \left[\frac{\partial W}{\partial x} \frac{\partial W}{\partial y} \right]; \; \tau_{xz} = \mu_t \frac{\partial W}{\partial x}; \; \tau_{yz} = \mu_t \frac{\partial W}{\partial y} \tag{9}$$

The following differences for the normal tensions of Reynolds are presented and used in order to predict the anisotropy in turbulent flow at non circular ducts,

$$\left(\tau_{yy}-\tau_{xx}\right)=c_{1NL}\mu_t\frac{k}{\varepsilon}\left[\left(\frac{\partial W}{\partial y}\right)^2-\left(\frac{\partial W}{\partial x}\right)^2\right] \tag{10}$$

Therefore, the Equation (6), including the tensions of Reynolds given in Equation (9), the turbulence production term is expressed as:

$$P_k=\tau_{xz}\frac{\partial W}{\partial x}+\tau_{yz}\frac{\partial W}{\partial y} \tag{11}$$

2.2.2. Reynolds Stress Model (RSM)

The most complex turbulence model is the Reynolds Stress Model (RSM), also known as second order model. It involves calculations of Reynolds stresses to an individual form, $\overline{\rho u_i' u_j'}$. These Reynolds stresses are used for formulating the differential equations of turbulent flow transport. The individual Reynolds stresses are utilized to close the average Reynolds equations of the momentum conservation. This model has shown superiority in relation to the two equation models (for example, $k-\varepsilon$) in simulating of complex flows that involve swirl, rotation, etc. The exact transport equations for the Reynolds stresses, $\overline{\rho u_i' u_j'}$, can be written as:

$$\begin{aligned}&\frac{\partial}{\partial t}(\rho\overline{u_i'u_j'})(a)+\frac{\partial}{\partial x_k}(\rho u_k\overline{u_i'u_j'})(b)=-\frac{\partial}{\partial x_k}\left[\rho\overline{u_i'u_j'u_k'}+\overline{p(\delta_{kj}u_i'+\delta_{ik}u_j')}\right](c)+\\&\frac{\partial}{\partial x_k}\left[\mu\frac{\partial}{\partial x_k}(\overline{u_i'u_j'})\right](d)-\rho\left(\overline{u_i'u_k'}\frac{\partial u_j}{\partial x_k}+\overline{u_j'u_k'}\frac{\partial u_i}{\partial x_k}\right)(e)-\rho\beta\left(g_i\overline{u_j'\theta}+g_j\overline{u_i'\theta}\right)(f)+\\&\overline{p\left(\frac{\partial u_i'}{\partial x_j}+\frac{\partial u_j'}{\partial x_i}\right)}(g)-2\mu\overline{\frac{\partial u_i'}{\partial x_k}\frac{\partial u_j'}{\partial x_k}}(h)-2\rho\Omega_k\left(\overline{u_j'u_m'}\varepsilon_{ikm}+\overline{u_i'u_m'}\varepsilon_{jkm}\right)(i)+S(j)\end{aligned} \tag{12}$$

Where the letters represent: (a) Local derivative of the time; (b) $C_{ij}\equiv$ Convection; (c) $D_{T,ij}\equiv$ Turbulent diffusion; (d) $D_{L,ij}\equiv$ Molecular diffusion; (e) $P_{ij}\equiv$ Production term of stresses; (f) $G_{ij}\equiv$ Buoyancy production term; (g) $\phi_{ij}\equiv$ Pressure-stress (redistribution); (h) $\varepsilon_{ij}\equiv$ Dissipation term; (i) $F_{ij}\equiv$ Production term for the rotation system; (j) $S_j\equiv$ Source term. The terms of the exact equations presented previously, C_{ij}, $D_{L,ij}$, P_{ij} and F_{ij} do not require modeling. However, the terms $D_{T,ij}$, G_{ij}, ϕ_{ij} and ε_{ij} need to be modeled to close the equations. For the present analysis, the model LRR (Launder, et al [37]) is chosen, which assumes that the correlation of velocity- pressure is a linear function of anisotropy tensor in the phenomenology of the redistribution, ϕ_{ij}. For the wall treatment, it is also assumed the Low Reynolds numbers and periodic conditions in according to Rokni [16]. This model had been simulated in the commercial code Fluent 6.3.

2.3 Turbulence models for turbulent heat flux

2.3.1. Simple Eddy Diffusivity (SED)

This method is based on the Boussinesq viscosity model. The turbulent diffusivity for the energy equation can be expressed as: $\alpha_t = \mu_t / \rho\sigma_t$, where the turbulent Prandtl number, σ_t for the SED model assumes a value constant in the entire region. For the air, σ_t it assumes a value equal to 0.89. The turbulent heat flux is given by,

$$\overline{\rho u_j t} = -\frac{\mu_t}{\sigma_T}\frac{\partial T_f}{\partial x_j} \tag{13}$$

2.3.2. Generalized Gradient Diffusion Hypothesis (GGDH)

Daly and Harlow [38] present the following formulation to the turbulent heat flux:

$$\overline{\rho u_j t} = -\rho C_t \frac{k}{\varepsilon}\left(\overline{u_j u_k}\frac{\partial T_f}{\partial x_k}\right) \tag{14}$$

The constant C_t, assumes the value of 0.3. The main advantage of this model is in considering the anisotropic behavior of the fluid heat transport in ducts.

2.3.3. Dimensionless energy equation for SED and GGDH models

For a given cross section of area "A", it is possible to define a mean velocity "U_b" and a bulk temperature "T_b", expressed as:

$$U_b = \frac{1}{A}\iint W.dx.dy \tag{15}$$

and

$$T_b = \frac{\int_A W.T_f.dA}{U_b.A} = \frac{1}{A.U_b}\iint W.T_f.dx.dy \tag{16}$$

Kays and Crawford [30] developed a formulation to rectangular cross section ducts. They considered the boundary conditions with prescribed uniform wall temperatures at the cross section, and at the duct length. According to Garcia [31], it is possible to carry out an analysis with non-uniform wall temperature boundary conditions. In this case, it is necessary to define a value that represents the mean wall temperatures in a given cross section, "T_{Wm}", given as:

$$T_{Wm} = \frac{\left[\frac{1}{L}.\int_0^L T_1(0,y).dy + \frac{1}{D}.\int_0^D T_2(x,0).dx + \frac{1}{L}.\int_0^L T_3(D,y).dy + \frac{1}{D}.\int_0^D T_4(x,L).dx\right]}{2(L+D)} \tag{17}$$

It is possible to develop a formula similar to Kays and Crawford [30], and a new expression for the turbulent energy equation can be presented as:

$$U\frac{\partial T_f}{\partial x} + V\frac{\partial T_f}{\partial y} + W\frac{\partial T_f}{\partial z} - \left[\frac{\partial}{\partial x}\left(\alpha\frac{\partial T_f}{\partial x} - \overline{ut}\right) + \frac{\partial}{\partial y}\left(\alpha\frac{\partial T_f}{\partial y} - \overline{vt}\right) + \frac{\partial}{\partial z}\left(\alpha\frac{\partial T_f}{\partial z} - \overline{wt}\right)\right] = 0 \tag{18}$$

The following considerations are applied to obtain the variables in dimensionless form:

$$X = \frac{x}{D_h}, \tag{19}$$

$$Y = \frac{y}{D_h} \tag{20}$$

and

$$\phi = \frac{\alpha.\left(T_{Wm} - T_f\right)}{U_b.D_h^2.\left(\frac{dT_b}{dz}\right)} \tag{21}$$

Replacing the Equations (13) or (14), (19)-(21) in Equation (18), dimensionless energy equations for SED and GGDH are obtained, respectively, expressed as:

$$\frac{\partial}{\partial X}\left\{(\alpha+\alpha_t)\frac{\partial\phi}{\partial X}\right\} + \frac{\partial}{\partial Y}\left\{(\alpha+\alpha_t)\frac{\partial\phi}{\partial Y}\right\} - (D_h)\left(U\frac{\partial\phi}{\partial X} + V\frac{\partial\phi}{\partial Y}\right) = -\frac{W}{U_B}\alpha\left(\frac{\phi}{\phi_B}\right) \tag{22}$$

$$\frac{\partial}{\partial X}\left[(\alpha_{ex})\frac{\partial\phi}{\partial X}\right] + \frac{\partial}{\partial Y}\left[(\alpha_{ey})\frac{\partial\phi}{\partial Y}\right] - D_h\left(U\frac{\partial\phi}{\partial X} + V\frac{\partial\phi}{\partial Y}\right) = -\frac{W}{U_B}\alpha\left(\frac{\phi}{\phi_B}\right) - C_t\frac{\partial}{\partial X}\left[\Gamma_X\frac{\partial\phi}{\partial Y}\right] - C_t\frac{\partial}{\partial Y}\left[\Gamma_Y\frac{\partial\phi}{\partial X}\right] \tag{23}$$

The fluid temperature field "T_f" can be replaced by "T_b" and the Equation (21) can be expressed as:

$$\phi_b = \frac{\alpha.\left(T_{Wm} - T_b\right)}{U_b.D_h^2.\left(\frac{dT_b}{dz}\right)}, \tag{24}$$

and

$$T_b = T_{Wm} - \frac{D_h^2.U_b}{\alpha}.\frac{dT_b}{dz}.\phi_b \tag{25}$$

From Equation (21), the Equation (26) is obtained, and applying this in Equation (16), the bulk temperature is obtained and expressed in Equation (27):

$$T_f = T_{Wm} - \frac{\phi.U_b.D_h^2.\left(\frac{dT_b}{dz}\right)}{\alpha}, \tag{26}$$

and

$$T_b = T_{Wm} - \frac{D_h^2}{\alpha.A}.\frac{dT_b}{dz}.\iint W.\phi.dx.dy \tag{27}$$

Replacing Equation (27) in Equation (24), and using Equations (19) and (20), the dimensionless bulk temperature is given as:

$$\phi_b = \frac{D_h^2}{A.U_b}.\iint W.\phi.dX.dY \tag{28}$$

It is possible to compute the heat transfer rate per unit length on the wall surface, " q' ", as shown in Equation (29) in function of "T_{Wm}", "T_b", and the average heat convection coefficient, " $\bar{h}$ ". From fluid enthalpy derivative gradient [$dh_b = c_p.dT_b$], the heat transfer rate per unit length in the fluid, " q'_f ", can be expressed by Equation (30).

$$q' = P_e.\bar{h}.(T_{Wm} - T_b), \tag{29}$$

and

$$q'_f = \rho.U_b.A.c_p.\frac{dT_b}{dz} \tag{30}$$

Equation (30) can be integrated to two cross sections (inlet, z_1, and outlet, z_2), thus, the following expression is obtained,

$$T_{b_{z2}} = T_{Wm} - \left(T_{Wm} - T_{b_{z1}}\right).e^{-\left(\frac{P_e}{2A}\right)^2.\frac{\alpha}{U_b}.Nu.\left(z_1 - z_2\right)} \tag{31}$$

From Equation (31), the bulk temperature longitudinal (*z-axis*) variation "ΔT_b" is obtained. It is done by "cutting" the duct into a lot of segments and applying the numerical method to find "ΔT_b" at each finite cross section. For a given bulk temperature at the duct inlet section (T_{b1}), after solving the equation system, duct outlet bulk temperature (T_{b2}) is calculated from Equation (31). The Dimensionless boundary conditions are given by the following equations:

$$\phi(0,Y)=\frac{\alpha.\left(T_{Wm}-T_1\right)}{U_b.D_h^2.\left(\frac{dT_b}{dz}\right)} \tag{32a}$$

and

$$\phi(X,0)=\frac{\alpha.\left(T_{Wm}-T_2\right)}{U_b.D_h^2.\left(\frac{dT_b}{dz}\right)} \tag{32b}$$

$$\phi(^{D}\!/_{D_h},Y)=\frac{\alpha.\left(T_{Wm}-T_3\right)}{U_b.D_h^2.\left(\frac{dT_b}{dz}\right)},\ \text{and}\ \ \phi(X,\tfrac{L}{D_h})=\frac{\alpha.\left(T_{Wm}-T_4\right)}{U_b.D_h^2.\left(\frac{dT_b}{dz}\right)} \tag{33}$$

When considering uniform wall temperature, the Equations (32) and (33) are equal to zero, and for these particular conditions, it is possible to notice that these boundary conditions are not functions of "dT_b/dz". That simplification becomes equal to the one studied by Patankar [32]. Equations (24)-(26) , as well as the boundary conditions from Equations (32) and (33), form a set of differential equations, in which "ϕ" and "dT_b/dz" parameters are unknown. When that equation system is solved, it is possible to obtain "T_f".

2.3.4. Additional equations

Additional equations were utilized for the calculation of the factor of friction Moody, f; coefficient of friction Fanning, C_f; Prandtl law; local Nusselt number for the Low Reynolds formulation (Rokni [16]), Nu_{xp} and Correlation of Gnielinsky, respectively. Thus, the additional equations are given by the following equations:

$$f\equiv\frac{-\left(dP/dz\right).D_h}{\rho U_B^2/2}, \tag{34}$$

$$C_f=\frac{f}{4} \tag{35}$$

$$\frac{1}{\sqrt{f}}=2\log\left(\mathrm{Re}\sqrt{f}\right)-0.8, \tag{36}$$

$$Nu_{xp}=D_h\frac{\left(T_w-T_P\right)}{\eta\left(T_w-T_b\right)} \tag{37}$$

$$Nu = \left[\frac{(f/8)(\mathrm{Re}-1000)\mathrm{Pr}}{\left(1+12.7(f/8)^{1/2}\left(\mathrm{Pr}^{2/3}-1\right)\right)} \right] \tag{38}$$

3. Numerical implementation

After applying the method of finite differences to the algebraic equations, to obtain the temperature fields, the following five steps indicate the developed methodology in the numerical solution. (Garcia [31]):

Step 1. To define the function value of the non uniform temperatures in the walls of the duct $T_{Wm} = f\left(T_1(0,y), T_2(x,0), T_3(D,y), T_4(x,L)\right)$, This function can be expressed by a Fourier expansion;

Step 2. To obtain velocity field and estimated values for "U_b" "T_{Wm}" *and* "dT_b/dz";

Step 3. Equations for the boundary conditions are evaluated (Equations 32 and 33);

Step 4. Dimensionless energy equation (Temperature field, "$Ø$") the Equation (23) is solved and "$Ø_b$" is computed according to Equation (28), until convergence is obtained ($Ø_b$ < tolerance). This is the end of the first iterative loop;

Step 5. A value for "dT_b/dz" is computed in accordance with Equation (25). Boundary conditions are updated (step 3) to obtain a solution for the new temperature field (step 4), until convergence is obtained (dT_b/dz < tolerance). This is the end of the second iterative loop;

For all steps, "tolerance of 10^{-7}" is the value to be accomplished by the convergence criteria, which is applicable to "$Ø_b$" (dimensionless bulk temperature), "dT_b/dz" and "$Ø$" (dimensionless temperature field).

4. Results and discussion

4.1. Fluid flow and heat transfer field

The Figure 2(a) shows the utilized grid (120X120) in the numerical simulation for the formulations of Low Reynolds, the Figure 2(b) it represents the secondary flow contours and comparisons of the velocity profile (NLEVM, Assato [8]) with the experimental work of the Melling and Whitelaw [5] for fluid water and Re=42000.

The predicted distributions of the friction coefficient (NLEVM and RSM) and Nusselt number (SED and GGDH) dependence on Reynolds number for fully developed flow and heat transfer in a square duct is shown in Figure 3(a) and 3(b), respectively.

Figure 4(a): comparisons of the Results (RSM-SED) numerical with the experimental for temperature profile (wall constant temperature) $(T_{Wm} - T_f)/(T_{Wm} - T_C)$ with fluid air and *Re*=65000 (Hirota [15]) are shown, the figure 4(b) shows the variation of the temperature

profile with non-uniform wall Temperature: south=400K, north=373K, east=393K, west=353K; presented as Case I.

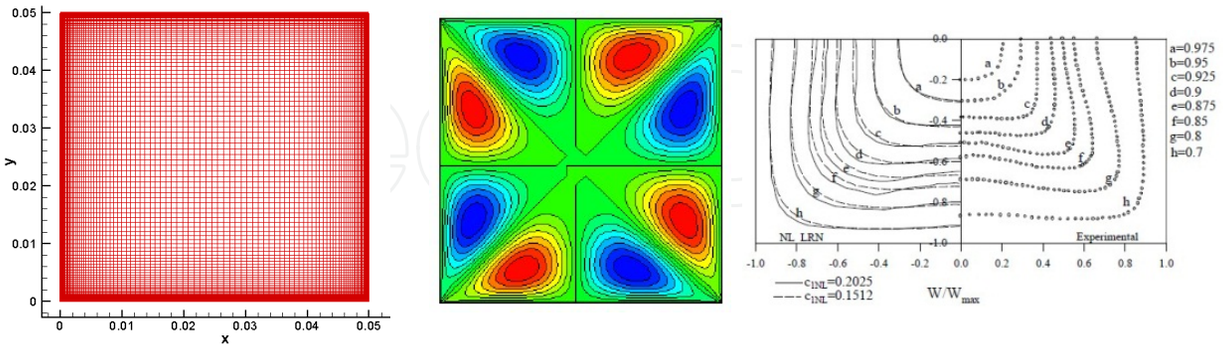

(a) (b)

Figure 2. (a) Grid 120X120 for numerical simulation (b) Secondary flow contours and comparisons of the axial mean velocity with Melling and Whitelaw [5] for water utilizing NLEVM Model.

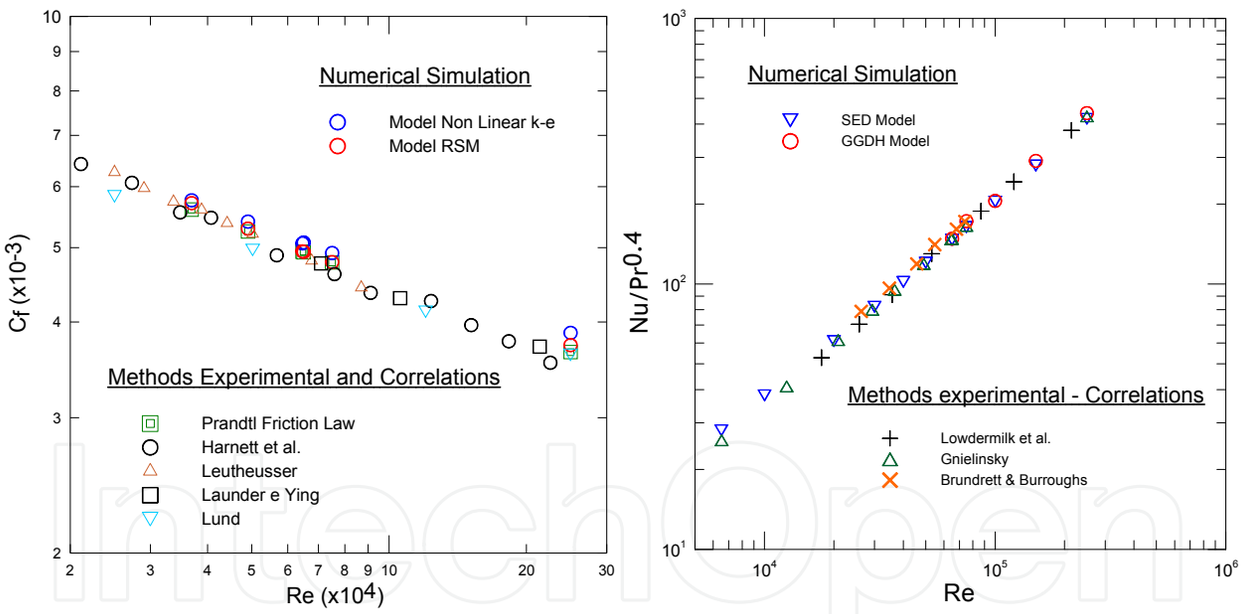

(a) (b)

Figure 3. (a) Friction coefficient for fully developed flow, (b) Nusselt number dependence on Reynolds number for fully developed flow

Already the Figure 5(a) shows: The variation of the temperature profile with non-uniform wall temperature, represented by means of functions sine (Case II), south=(350-20Sin(ζ))K, north=(400-50Sin(ζ))K, east=(330+20Sin(ζ))K, west=(350+50Sin(ζ))K. where ζ is function of the radians (0-π/2) and *i,j* (points number of the grid in the direction x and y, respectively). The Figure 5(b) shows the behavior of the "T_b" and "*DTb/dz*" for different square cross sections in the direction of the main flow, according to Equation (31).

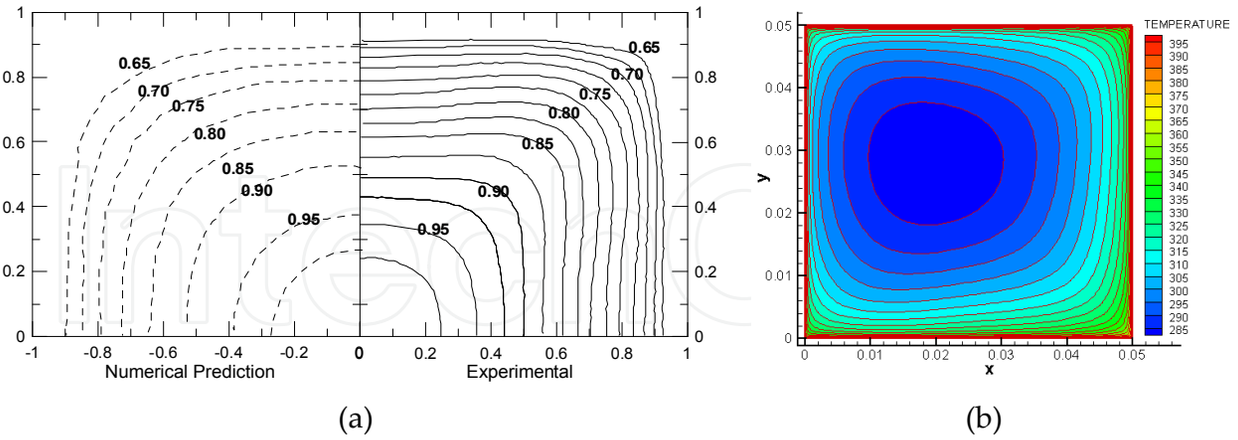

Figure 4. (a) Results (RSM-SED) numerical and (Hirota et al [15]) experimental for mean temperature (uniform wall temperature) (b) Fluid temperature with non-uniform wall Temperature (Case I).

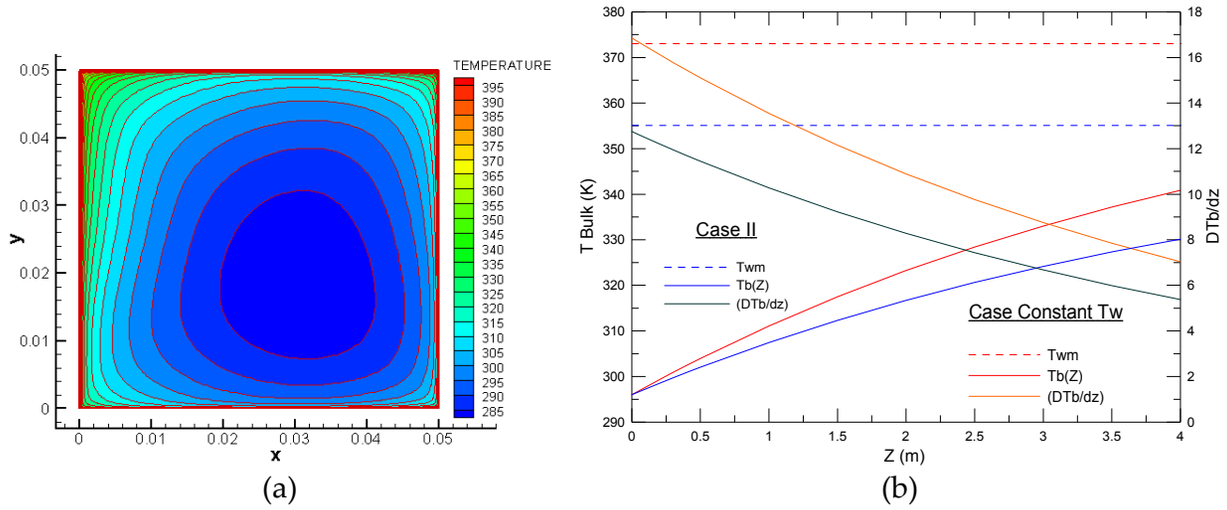

Figure 5. (a) Fluid temperature with non-uniform wall temperature (Case II) (b) Behavior "T_b" for different square cross sections and cases in the direction of the main flow.

The Figures 6 (a) and (b), shown the temperature distribution for a rectangular duct aspect ratio (1:2) represented by means of a function sine (Case II). A third case denominated Case III is represented by: south= $405+10\left[\frac{\text{nx-1}}{\text{nx}_{\text{máx}}-1}\right]$ *K*; North= $395+10\left[\frac{\text{nx-1}}{\text{nx}_{\text{máx}}-1}\right]$ *K*; east= 405-10 $\left[\frac{\text{ny-1}}{\text{ny}_{\text{máx}}-1}\right]$ *K;* west= $415-10\left[\frac{\text{ny-1}}{\text{ny}_{\text{máx}}-1}\right]$ *K. S*ome results for rectangular ducts are shown in the Table 1.

In the doctoral thesis Garcia (1996) was analyzed the laminar flow coupled to the conduction and radiation in rectangular ducts and concluded that as increases the aspect ratio, the Nusselt number found in the coupling, differs from that found for ducts with

constant temperature imposed around the perimeter of the section. which shows that could be making a mistake to consider the literature results without calculating the energy equation.

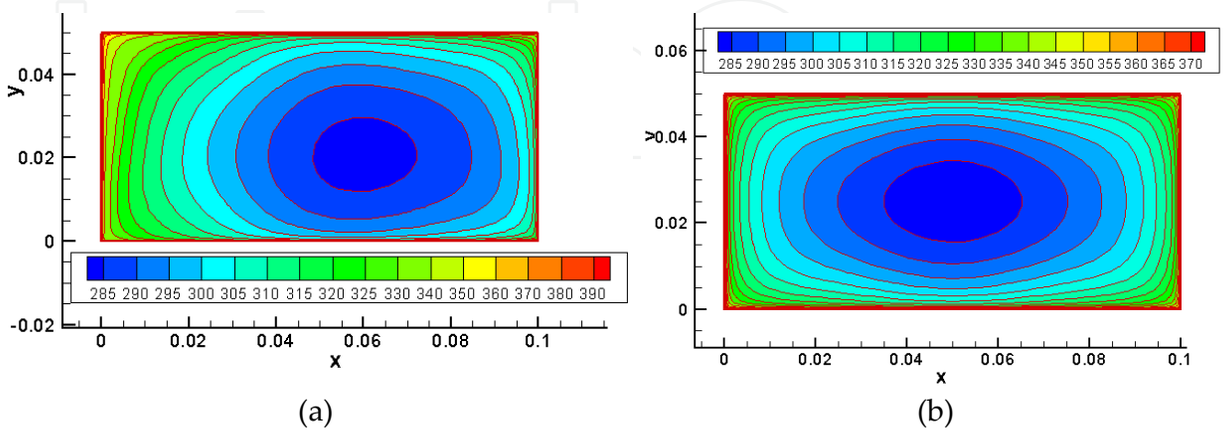

Figure 6. (a) Retangular duct aspect ratio (1:2) case II, Re=65000 with *Tb*=300 *K*, utilizing the SED model (b) Retangular duct aspect ratio (1:2) with constant temperature in the perimeter *Twm*=373 *K*, *Re*=65000 with *Tb*=300 *K*, utilizing the SED model.

In the present study, the variations of the average Nusselt number for a square duct and different cases analyzed (uniform and non uniform temperature in the perimeter) are minimal. Already in the case of rectangular duct with an aspect ratio (1:2), the variations should be taken into account as shown in Table 1.

Cases Analyzed	Reynolds number (Re)	Nusselt number calculated *(Nu)*	Correlation Dittus Boelter *(Nu)*.
Temperature Constant	65000	145, 910	142,89
Case II	65000	139, 682	-
Case III	65000	145, 059	-
Temperature Constant	28853	79, 101	77,1
Case III	28853	76, 769	-

Table 1. Numerical results obtained through RSM-SED model [34], for the averaged Nusselt number in a rectangular duct with aspect ratio (1:2).

5. Conclusions

The results shown what for the friction factor and Nusselt number in a wide range of the Reynolds number with uniform wall temperature have a reasonable approach with the

experimental works and correlation of the literature, (Figure 3(a), (b)). The Figures 4(b) and 5(a) shown new results investigated in present study, which is observed a distortion of the temperatures field and as consequence a variation of the Nusselt number caused mainly by the distribution of the non-uniform wall temperature (Case I and II, with fluid air and *Re*=65000, respectively). Most applications can be approximated by the functions sine and cosine in the wall, but we are able to resolve by means of the methodology presented, any peripheral heat flux variation that can be expressed by a Fourier expansion (Kays and Crawford [30]). The Figure 5(b) shows the comparisons of the behavior of the curves "T_b" and "*DTb/dz*" in the direction of the main flow for Case II and Case uniform wall temperature. The variations of the average Nusselt number for a square duct and different cases analyzed (uniform and non uniform temperature in the perimeter) are minimal. Already in the case of duct with an aspect ratio (1:2) the variations should be taken into account. These results can be helpful in the project of thermal devices as in heat transfer and secondary flows in cavities, seals, channel of gas turbines and others.

Nomenclature

C_{ij} convection
c_p specific heat at constant pressure
D duct height
D_h hydraulic diameter, $D_h = 4.A/P_e = 2.L.D/(L+D)$
$D_{L,ij}$ molecular diffusion
$D_{T,ij}$ Turbulent diffusion
dP/dz pressure gradient at z direction (longitudinal axis)
f, C_f factor of Moody´s friction, and Fanning´s friction coefficient, respectively.
F_{ij} Term production for the rotation system
G_{ij} buoyancy production Term
k_f fluid thermal conductivity
L duct width
Nu Nusselt number
P_e perimeter
P_{ij} production Term of tensions
P_k turbulence production term
Re Reynolds number
S_j Source term
T temperature
T_b internal flow bulk temperature
T_{Wm} wall mean temperature
T_1, T_2, T_3 and T_4 temperature distributions at duct wall (bottom, right side, top and left side)
U_b internal flow bulk velocity
U, V and W average velocity in the direction x, y and z; respectively
y^+ dimensionless wall distance

Greek Symbols

α	thermal diffusivity, $\alpha = k_f / (\rho . c_p)$
ε_{ij}	Term of dissipation
η	distance normal to the wall
ϕ	dimensionless temperature distribution
ϕ_{ij}	Term of pressure-tension (redistribution)
μ	dynamic viscosity
μ_t	turbulent viscosity
ρ	density
σ_t	turbulent Prandtl number

Author details

G.A. Rivas*, E.C. Garcia and M. Assato
Instituto Tecnologico de Aeronautica (ITA),Brazil

6. References

[1] Z.H. Qin; R.H. Plecther, Large eddy simulation of turbulent heat transfer in a rotating square duct, International Journal Heat Fluid Flow. 27 (2006) 371-390.

[2] J. Nikuradse, 1926, Untersuchung uber die Geschwindigkeitsverteilung in turbulenten Stromungen, Diss. Göttingen, VDI - forschungsheft 281.

[3] F.B. Gessner and A.F. Emery, A Reynolds stress model for turbulent corner flows – Part I: Development of the model, Journal Fluids Eng. 98 (1976) 261-268.

[4] F.B. Gessner, and J.K. Po, A Reynolds stress model for turbulent corner flows – Part II: Comparison between theory and experiment, Journal Fluids Eng. 98 (1976) 269-277.

[5] A. Melling and J.H. Whitelaw, Turbulent flow in a rectangular duct, Journal Fluid Mechanical. 78 (1976) 289-315.

[6] A. Nakayama, A.; W.L. Chow and D. Sharma, Calculation of fully development turbulent flows in ducts of arbitrary cross-section, Journal Fluid Mechanical, 128 (1983) 199-217.

[7] H.K. Myon and T. Kobayashi, Numerical Simulation Of Three Dimensional Developing Turbulent Flow in a Square Duct with the Anisotropic κ-ε Model, Advances in Numerical Simulation of Turbulent Flows ASME, Fluids Engineering Conference, 1991. Vol.117, Portland, United States of America, pp. 17-23.

[8] M. Assato, Análise numérica do escoamento turbulento em geometrias complexas usando uma formulação implícita, Doctoral Thesis, Departamento de Engenharia

* Corresponding Author

Mecânica, Instituto Tecnológico de Aeronáutica - ITA, São José dos campos - SP, Brazil, 2001.

[9] M. Assato; M.J.S. De Lemos, Turbulent flow in wavy channels simulated with nonlinear models and a new implicit formulation, Numerical Heat Transfer – Part A: Applications. 56 (4) (2009) 301-324.

[10] D. Home; M.F. Lightstone; M.S. Hamed, Validation of DES-SST based turbulence model for a fully developed turbulent channel flow problem, Numerical Heat Transfer – Part A: Applications. 55 (4) (2009) 337-361.

[11] D. D. Luo; C.W. Leung; T.L. Chan; W.O. Wong, Simulation of turbulent flow and forced convection in a triangular duct with internal ribbed surfaces, Numerical Heat Transfer – Part A: Applications. 48 (5) (2005) 447-459.

[12] S. Ergin; M. Ota; H. Yamaguchi, Numerical study of periodic turbulent flow through a corrugated duct, Numerical Heat Transfer – Part A: Applications. 40 (2) (2001) 139-156.

[13] B.E. Launder and W.M.Ying., Prediction of flow and heat transfer in ducts of square cross section", Proc. Inst. Mech. Eng., 187 (1973) 455-461.

[14] A.F. Emery, P.K. Neighbors and F.B. Gessner, The numerical prediction of developing turbulent flow and heat transfer in a square duct, Journal Heat Transfer, 102 (1980) 51–57.

[15] M. Hirota, H. Fujita, H. Yokosawa, H. Nakai, H. Itoh, Turbulent heat transfer in a square duct, International Journal Heat and fluid flow, 18 (1997) 170-180.

[16] M. Rokni, Numerical investigation of turbulent fluid flow and heat transfer in complex duct, Doctoral Thesis, Department of Heat and Power Engineering. Lund Institute of Technology, Sweden, 1998.

[17] Y. Hongxing, Numerical study of forced turbulent heat convection in a straight square duct, International Journal of Heat and Mass Transfer, 52 (2009) 3128-3136.

[18] Y.T. Yang; M.L. Hwang, Numerical simulation of turbulent fluid flow and heat transfer characteristics in a rectangular porous channel with periodically spaced heated blocks, Numerical Heat Transfer – Part A: Applications. 54 (8) (2008) 819-836.

[19] T.S. Park, Numerical study of turbulent flow and heat transfer in a convex channel of a calorimetric rocket chamber, Numerical Heat Transfer – Part A: Applications. 45 (10) (2004) 1029-1047.

[20] J. Zhang; L. Dong; L. Zhou; S. Nieh, Simulation of swirling turbulent flows and heat transfer in a annular duct, Numerical Heat Transfer – Part A: Applications. 44 (6) (2003) 591-609.

[21] B. Zheng; C.X. Lin; M.A. Ebadian, Combined turbulent forced convection and thermal radiation in a curved pipe with uniform wall temperature, Numerical Heat Transfer – Part A: Applications. 44 (2) (2003) 149-167.

[22] J. Su; A.J. Da Silva Neto, Simultaneous estimation of inlet temperature and wall heat flux in turbulent circular pipe flow, Numerical Heat Transfer – Part A: Applications. 40 (7) (2001) 751-766.

[23] A. Saidi; B. Sundén, Numerical simulation of turbulent convective heat transfer in square ribbed ducts, Numerical Heat Transfer – Part A: Applications. 38 (1) (2001) 67-88.

[24] M. Rokni, A new low-Reynolds version of an explicit algebraic stress model for turbulent convective heat transfer in ducts, Numerical Heat Transfer – Part B: Fundamentals. 37 (3) (2000) 331-363.

[25] A. Valencia, Turbulent flow and heat transfer in a channel with a square bar detached from the wall, Numerical Heat Transfer – Part A: Applications. 37 (3) (2000) 289-306.

[26] M.C. Sharatchandra; D.L. Rhode, Turbulent flow and heat transfer in staggered tube banks with displaced tube rows, Numerical Heat Transfer – Part A: Applications. 31 (6) (1997) 611-627.

[27] A. Campo; K. Tebeest; U. Lacoa; J.C. Morales, Application of a finite volume based method of lines to turbulent forced convection in circular tubes, Numerical Heat Transfer – Part A: Applications. 30 (5) (1996) 503-517.

[28] M. Rokni; B. Sundén, Numerical investigation of turbulent forced convection in ducts with rectangular and trapezoidal cross section area by using different turbulence models, Numerical Heat Transfer – Part A: Applications. 30 (4) (1996) 321-346.

[29] G. Yang; M.A. Ebadian, Effect of Reynolds and Prandtl numbers on turbulent convective heat transfer in a three-dimensional square duct, Numerical Heat Transfer – Part A: Applications. 20 (1) (1991) 111-122.

[30] W.M. Kays; M.Crawford, Convective Heat and Mass Transfer, McGraw-Hill, New York, USA, 1980, pp. 250-252.

[31] E.C. Garcia, Condução, convecção e radiação acopladas em coletores e radiadores solares, Doctor degree thesis, ITA - Instituto Tecnológico de Aeronáutica, São José dos Campos, SP, Brasil, 1996.

[32] S.V. Patankar, Computation of Conduction and Duct Flow Heat Transfer, Innovative Research, Maple Grove, USA, 1991.

[33] M.J. Moran, et al, Introdução à Engenharia de Sistemas Térmicos: Termodinâmica, Mecânica dos Fluidos e Transferência de Calor, LTC Ed., Rio de Janeiro-RJ, Brasil, 2005.

[34] G. A. Rivas Ronceros, Simulação numérica da convecção forçada turbulenta acoplada à condução de calor em dutos retangulares, Doctor degree thesis, ITA - Instituto Tecnológico de Aeronáutica, São José dos Campos, SP, Brasil, 2010.

[35] C. G. Speziale, On Nonlinear k-ε and k-l Models of Turbulence, J. Fluid Mech., vol. 176, pp. 459-475, 1987.

[36] K. Abe, et al, An Improved k-ε Model for Prediction of Turbulent Flows with Separation and Reattachment, Trans. JSME, Ser. B, vol. 58, pp. 3003-3010, 1992.

[37] B.E. Launder, G.J. Reece, and W. Rodi: Progress in the development of a Reynolds-stress turbulence closure, J. Fluid Mech., vol.68, 537-566, 1975.

[38] Daly and Harlow: transport equations in turbulence, Phys. Fluids., vol.13, 2634-2649, 1970.

IntechOpen